# Parametric equations for the variables of a steady-state model of a multi-effect desalination plant

**Patricia Palenzuela*, Diego Alarcón, Guillermo Zaragoza, Julián Blanco, Mercedes Ibarra**

CIEMAT-Plataforma Solar de Almería, Ctra. de Senés s/n, 04200 Tabernas, Almería, Spain.

*Corresponding author. Tel.: +34 950387909; fax: +34 950365015. *Email address*: patricia.palenzuela@psa.es

*Email addresses*: patricia.palenzuela@psa.es, diego.alarcon@psa.es, guillermo.zaragoza@psa.es, julian.blanco@psa.es, , mercedes.ibarra@psa.es

**Abstract**

In the present work a steady-state model is developed of an MED plant. Its development and validation have been carried out by experimental data obtained from an MED pilot plant located at the Plataforma Solar de Almería (PSA), in the southeast of Spain. It is a vertical-arrangement forward-feed MED plant with pre-heaters, which uses hot water as the thermal energy source. In order to run the model a series of parametric equations for these variables: the overall heat transfer coefficient for the first effect ($U_h$), the overall heat transfer coefficient for the pre-heaters ($U_p(i)$), the vapor temperature inside the first effect, ($T_v(1)$) and the cooling seawater outlet temperature ($T_{cwout}$) have been determined. They have been obtained from a three-level factorial experimental design ($3^k$), performing a total of 81 experiments ($3^4$). The results obtained showed a good fit to the estimated models for the response variables.

*Keywords*: Solar desalination; Multi-effect distillation; Modeling

## 1. Introduction

Industrial desalination of seawater is one of the possible solutions to alleviate the worldwide scarcity of freshwater. The industrial desalination processes can be split into two main categories: (1) thermal processes which include multi-stage flash (MSF) and multi-effect distillation (MED) as the most commercially successful, and (2) membrane processes including reverse osmosis (RO). The advantages of thermal desalination processes are their ability to be driven by low exergy thermal sources, their reliability, easier operation and maintenance and high purity freshwater. Among the thermal desalination processes, MED has the highest thermal efficiency and the lowest power consumption [1]. However, the disadvantage of thermal desalination processes is that the overall energy consumption is high, so the use of renewable energies is required to guarantee the sustainability of this technological option [2, 3]. The usual coincidence in many locations of fresh water shortage, abundant seawater resources and high isolation levels makes thermal seawater desalination driven by solar energy as one of the most promising processes to obtain fresh water. This can be possible by the coupling of a conventional thermal distillation plant with a solar thermal system [4].

The improvement in the design of a MED process can be reached by the prediction of its performance over a wide range of operating conditions. Mathematical modeling and computer simulations can provide an insight into the workings of the system and help to understand in detail the process elements in order to predict the behavior and the efficiency of the system. Many papers have been published on the topic of modeling and simulation of MED processes. El-Dessouky et al. have made several contributions in the mathematical modeling of MED plants [5, 6]. El-Nashar et al. [7, 8] presented a mathematical simulation of the steady-state operation of a solar MED unit, which was validated with experimental data from a pilot plant located at Abu Dhabi, UAE. A computer simulation model of a multi-effect thermal vapour compression (TVC-MED) was presented by Kamali [9] to predict the influence of all factors on heat transfer coefficients, temperature and pressure, total capacity and performance ratio of the system under design and operating conditions. Also, Trostmann [10] developed a model and carried out steady state simulations of a MED-TVC, where heat

transfer coefficients correlations for condensation and evaporation in the tubes were discussed and compared. Gautami et al. [11] developed mathematical models in order to select the optimal configuration of a MED process based on product concentration and steam economy. Finally, the authors developed a model of an MED plant, based on the MED pilot plant located at the Plataforma Solar de Almería (PSA) [12]. To solve this model, a parameterization of the overall heat transfer coefficients was carried out by performing a series of experiments at the MED-PSA plant. The correlations obtained were based on the characterization published by El-Nashar [8].

In this paper, new correlations have been obtained by the authors by means of a parametric study. The parametric equations have been determined for these variables: the overall heat transfer coefficient for the first effect ($U_h$), the overall heat transfer coefficient for the pre-heaters ($U_p(i)$), the vapor temperature inside the first effect, ($T_v(1)$) and the cooling seawater outlet temperature ($T_{cw,out}$). Such parametric equations have been obtained using a factorial design.

## 2. Description of the plant

### *2.1 Process design*

The desalination plant at the PSA, with 14 cells or effects, is a forward-feed MED unit manufactured and delivered by ENTROPIE in 1987 [13]. The cells are in a vertical arrangement at decreasing pressures from cell 1 to cell 14 [14]. The first cell, which was modified in 2005 within the framework of a project called AQUASOL, works with hot water as the heat transfer media [15]. Originally, the first cell worked with low-pressure saturated steam (70ºC, 0.31 bars). The hot water for the first cell is provided either with a solar field composed of static compound parabolic concentrators (CPC) or with a double effect absorption heat pump, DEAHP (LiBr-$H_2O$) which was manufactured by ENTROPIE in 2005 in the framework of the AQUASOL project [16-18]. In the modelling developed in this paper, only the case in which the hot water comes from the solar filed has been taken into account.

The flow sheet of the process is shown in Fig 1. Firstly, the pumped feed seawater flows through the condenser and the pre-heaters of the plant in order to preheat it before reaching the first effect. Once in the first effect, the seawater is sprayed through a spraying tray falling over a horizontal-tube bundle. Then, it is built a thin falling film which coats the surface of the tubes entirely. On the other hand, the hot water flows inside the tubes and releases its sensible heat to the seawater, evaporating part of it. Vapor generated in the first effect flows to the pre-heater located next to it, through a wire mesh demister which removes the entrained brine droplets. Here, vapor transfers part of its latent heat to the seawater which is circulating inside the pre-heater bundle tube, increasing its temperature. As a consequence, a small amount of the vapor condenses, which is the first distillate of the process. The vapor which has not condensed flows through the inside of the second effect tube bundle, being the thermal energy source in the evaporation-condensation process in this effect. Then, the vapor condenses by transferring its latent heat to the more concentrated brine flowing from the previous effect.

The same process is repeated in the rest of effects, being the vapor produced in the previous effect the thermal energy source of the effect. In each effect, as in the first one, part of the vapor generated is used to preheat the seawater that flows through the pre-heaters. Finally, the vapor produced in the last effect is led to the end condenser, where is condensed by transferring the latent heat of evaporation to the cooling seawater which is passing through the condenser bundle tube. That heated seawater is divided into two streams, some is pumped to the first effect of the plant after passing through the pre-heaters of each effect and the rest is rejected.

The vapor condensed in each effect and in the pre-heaters together with the distillate from the last condenser make up the total distillate of the plant. In order to improve the process from an energetic point of view, the distillate produced in each effect goes to other effects of the plant to recover part of its sensible heat. In some cases, the distillate goes from an effect to the next one, and in other cases, it goes to further effects as follows: in the fourth cell all the distillate is extracted, part of it goes to the seventh cell and the rest to the tenth. Similar extraction is made in the seventh cell, splitting the condensate between the tenth and the thirteenth effects. Another extraction takes place from the tenth cell, part goes to the thirteenth effect and the rest is mixed with the distillate produced in the fourteenth effect. The final extraction is made in the thirteenth effect, after which all the distillate is mixed with that produced in the fourteenth effect. Finally, this accumulated distillate is mixed with the distillate from the condenser, making up the total production.

Besides the vapor formed by boiling, a small portion is formed by flashing. When the distillate and the brine pass from one effect to another, some flashing takes place since they enter a cell which is at a lower pressure than the previous one.

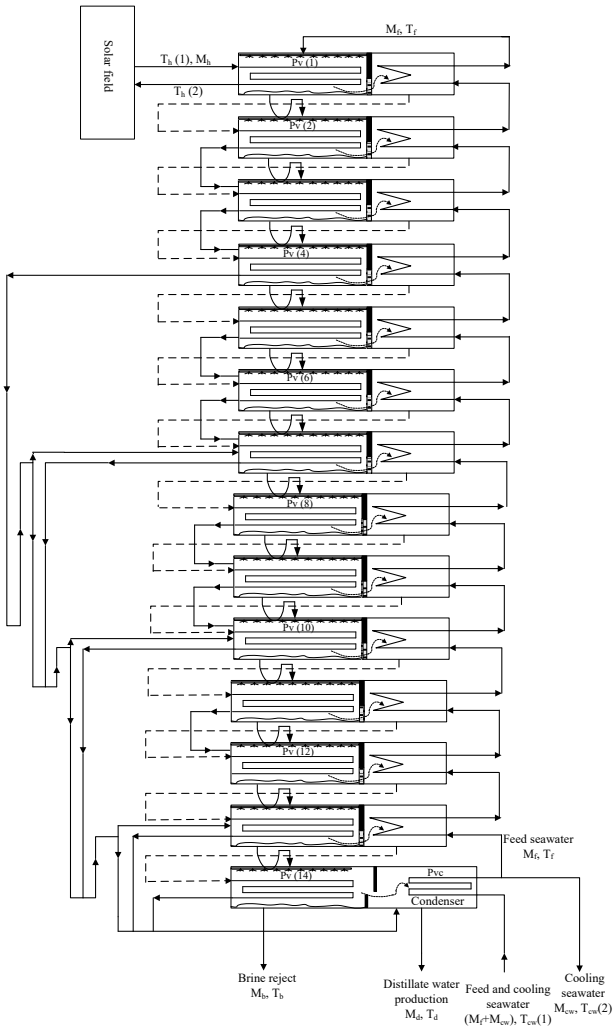


Fig 1. Schematic diagram of the multi-effect distillation plant at the Plataforma Solar de Almería. Dashed lines show the steam flow; solid lines the distillate flow; U-shaped lines represent the brine flow from one effect to the next.

The vacuum system consists of two hydro-ejectors, which are connected to effects 2, 7 and the end condenser. They are within a closed circuit with a tank and an electric pump that pumps seawater through the ejectors at a pressure of 3 bar. This vacuum system does the initial vacuum of the plant removing the air and the non-condensable gases generated during the desalination process.

The design specifications of the PSA MED plant are given in Table 1. The tube bundles of the heater, evaporators, pre-heater and condenser are made of 90-10 Cu-Ni tubes. The surface areas of each of the different tube bundles are:

- First effect evaporator bundle, 24.26 $m^2$.
- Effect 2-14 evaporator bundle, 26.28 $m^2$.
- Pre-heater bundle, 5 $m^2$.
- Condenser bundle, 18.3 $m^2$.

Table 1
Design specifications of the MED-PSA plant.

| | |
|---|---|
| Number of effects | 14 |
| Feed seawater flow rate | 8 $m^3/h$ |
| Brine flow rate from the last effect | 5 $m^3/h$ |
| Hot water flow rate | 12.0 L/s |
| Total distillate output | 3 $m^3/h$ |
| Cooling seawater flow rate at 25 ºC | 20 $m^3/h$ |
| Vapor production in the last effect at 70 ºC | 159 kg/h |
| Heat source energy consumption | 200 kW |
| Performance ratio | > 9 |
| Vacuum system | Hydro-ejectors (seawater at 3 bar) |
| Inlet/Outlet hot water temperature | 74.0/70.0 ºC |
| Brine temperature (on the first cell) | 68 ºC |
| Feed and cooling seawater temperature at the outlet of the condenser | 33 ºC |

*2.2 Experimental set-up*

The MED-PSA plant is experimental and therefore equipped with a comprehensive monitoring system, which provides instantaneous values of the measured data. The monitored data are detailed in Table 2 and are also indicated in Fig 1.

Table 2
Monitored data at PSA MED plant

| Measurement | Name of variable | Magnitude |
|---|---|---|
| **Flow rate:** | $M_h$ | Heating water flow |
| | $M_{cw}$ | Cooling seawater flow |
| | $M_f$ | Feed seawater flow |
| | $M_d$ | Product water flow |
| | $M_b$ | Brine flow |
| **Temperature:** | $T_{h,in}$ | Heating water inlet |
| | $T_{h,out}$ | Heating water outlet |
| | $T_f$ | 1st effect sprayed seawater temp. |
| | $T_{cw,in}$ | Cooling seawater inlet temp. |
| | $T_{cw,out}$ | Cooling seawater (rejected) outlet temp. |
| **Pressure:** | $P_v(1)$, $P_v(2)$, $P_v(4)$, $P_v(6)$, $P_v(8)$, $P_v(10)$, $P_v(12)$, $P_v(14)$ | 1st, 2th, 4th, 6th, 8th, 10th, 12th, 14th effect vapor press. |
| | $P_{h,in}$ | Heating water inlet pressure |
| | $P_{vc}$ | Vapor pressure in the condenser |
| **Salt concentration:** | $X_f$ | Seawater TDS at the condenser inlet |

The supply water to the desalination plant is obtained from wells and stored in a pool from where the cooling water is pumped to the bundle tube of the condenser. Afterwards, part of it is used as feed water in the first effect and the rest is rejected back to the pool. Therefore, part of the heat released at the condenser goes into the pool and the cooling water temperature could increase during the experiment, which is not desirable. To avoid that, a dry cooler is switched on since the beginning of the experiment cooling the pool.
As the model proposed is at steady-state, time averages of the measured data are carried out in order to perform the modeling.

## 3. Mathematical model

The model is based in steady state mass and energy balances, and the heat transfer equations for all the components of the plant, considering the work developed by El-Dessouky and Ettouney (2002). As opposed of the model of El-Dessouky, the first effect has been modeled taking into account that this unit uses hot water as the thermal energy source instead of vapor. The model has been implemented in MATLAB environment accounting for the processes and features of the MED-PSA plant. The following assumptions have been taken into account in order to simplify the analysis: steady state operation, negligible heat losses to the surroundings, equal temperature difference across the effects, equal temperature difference across the pre-heaters, salt-free distillate from all the effects, the condensate that leaves each effect is considered as saturated liquid.

To develop the model, the MED system has been divided into three blocks: the first effect, the effect 2 – N and the end condenser. Within the second block there are three sub-blocks: the first one, which consider the effects in which the distillate that enters comes from the previous effect and pre-heater (effects 3, 4, 6, 9 and 12), the effects in which the distillate that enters comes from the previous effect, from the preivous pre-heater and from further effects (effects 7, 10 and 13) and the effects in which the distillate that enters comes from the previous pre-heater (effects 2, 5, 8, 11 and 14). The first two blocks (the first effect and the effects 2 – N)

have two control volumes: the evaporator and the pre-heater. The evaporator is the part of the effect where the seawater is sprayed over the bundle tube and part of the brine is evaporated.

*3.1 The first effect*

Fig 2 shows a schematic diagram of the heater, which corresponds to the first effect of the plant.

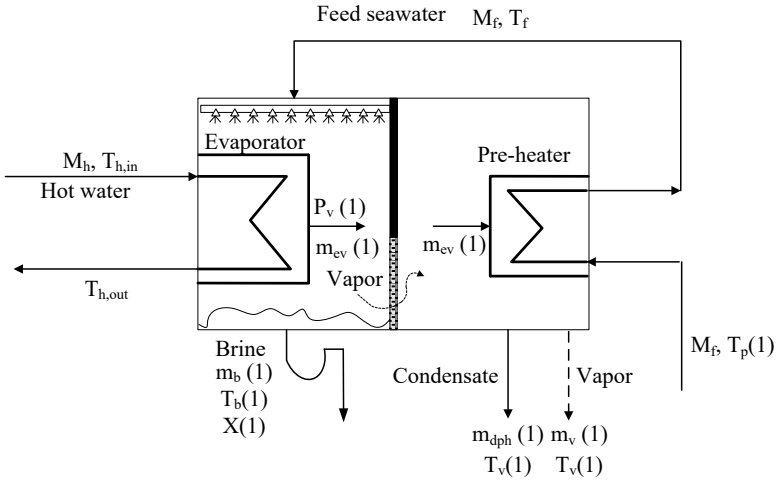


Fig 2. Flow diagram of the heater (effect 1)

The mass, salt and energy balances of the evaporator are the following:

- Energy balance:

$$M_h \cdot h_{h,in} + M_f \cdot h_f = m_{ev}(1) \cdot h_{ev}(1) + M_h \cdot h_{h,out} + m_b(1) \cdot h_b(1) \quad (1)$$

where $M_h$ is heating water mass flow rate from the solar field, $M_f$ is the feed seawater mass flow rate, mev(1) the vapor mass flow rate which leaves the evaporator, $m_b(1)$ the brine mass flow rate that leaves the first effect and $h$ is the enthalpy corresponding to each stream.

- Mass and salt balances:

$$M_f = m_b(1) + m_{ev}(1) \quad (2)$$

$$X_f M_f = X(1) \cdot m_b(1) \quad (3)$$

where $X_f$ is the feed seawater salinity and $X(1)$ the salinity of the brine that leaves the first effect.

The mass and energy balances of the pre-heater are the following:

- Energy balance:

$$m_{ev}(1) \cdot h_{ev}(1) + M_f \cdot h_p(1) = m_v(1) \cdot h_v(1) + m_{dph}(1) \cdot h_{dph}(1) + M_f \cdot h_f \quad (4)$$

- Mass balance:

$$m_{ev}(1) = m_v(1) + m_{dph}(1) \quad (5)$$

where $m_v(1)$ is the vapor mass flow rate which leaves the first pre-heater and $m_{dph}(1)$ is the distillate mass flow rate that is generated in the pre-heater.

It is considered that the condensate generated in the pre-heater and the rest of vapor leave the pre-heater at a temperature of $T_v(1)$ (it corresponds to the saturation pressure $P_v(1)$). This temperature is lower that of the boiling brine temperature ($T_b(1)$) by the boiling point elevation ($BPE$). Therefore:

$$T_b(1) = T_v(1) + \left(BPE\right)_1 \tag{6}$$

This parameter can be determined by a correlation published by El-Dessouky [19, 20], which is as follows:

$$\begin{aligned} &BPE(1) = A \cdot X(1) + B \cdot X(1)^2 + C \cdot X(1)^3 \\ &A = 8{,}325 \cdot 10^{-2} + 1{,}883 \cdot 10^{-4} \cdot T_b(1) + 4{,}02 \cdot 10^{-6} \cdot T_b(1)^2 \\ &B = -7{,}625 \cdot 10^{-4} + 9{,}02 \cdot 10^{-5} \cdot T_b(1) - 5{,}2 \cdot 10^{-7} \cdot T_b(1)^2 \\ &C = 1{,}522 \cdot 10^{-4} - 3 \cdot 10^{-6} \cdot T_b(1) - 3 \cdot 10^{-8} \cdot T_b(1)^2 \end{aligned} \tag{7}$$

where $X(1)$ is the salt weight percentage that leaves the first effect. The above equation is valid over the following ranges: $1 \le X(1) \le 16$ %, $10 \le T_b(1) \le 180$ °C.

The heat transfer equation for the evaporator of the first effect can be written as:

$$Q_h = A_h \cdot U_h \cdot \frac{\left(T_{h,in} - T_b(1)\right) - \left(T_{h,out} - T_b(1)\right)}{\ln\left(\dfrac{T_{h,in} - T_b(1)}{T_{h,out} - T_b(1)}\right)} \tag{8}$$

where $U_h$ is the overall heat transfer coefficient for the heater, $A_h$ is the first effect evaporator bundle tube, $T_{h,in}$ the heating water inlet temperature and $T_{h,out}$ the heating water outlet temperature. $Q_h$ is the thermal power that the hot water transfers to the seawater that is sprayed over the first effect, and it is defined as follows:

$$Q_h = M_h \cdot C_{ph} \cdot (T_{h,in} - T_{h,out}) \tag{9}$$

where $C_{ph}$ is the hot water specific heat.

In the case of the pre-heater, the heat transfer equation is given by:

$$Q_p(1) = A_p \cdot U_p(1) \cdot \frac{\left(T_v(1) - T_p(1)\right) - \left(T_v(1) - T_f\right)}{\ln\left(\dfrac{T_v(1) - T_p(1)}{T_v(1) - T_f}\right)} \tag{10}$$

where $U_p(1)$ is the overall heat transfer coefficient of the first pre-heater, $A_p$ is the pre-heater bundle (it is considered the same for all the pre-heaters), $T_p(1)$ is the seawater temperature in the inlet of the first pre-heater and $T_f$ is the seawater temperature in the outlet of the last pre-heater. $Q_p(1)$ is the thermal power that the vapor coming from the evaporator transfer to the seawater flowing through the tubes of the pre-heater and it is determined by this equation:

$$Q_p(1) = M_f \cdot C_{pf} \cdot T_f - M_f \cdot C_p(1) \cdot T_p(1) \tag{11}$$

where $C_p(1)$ and $C_{pf}$ are the seawater specific heat at the inlet of the first pre-heater and at the outlet of the last one, respectively.

*3.2 Effects 2-N*

As mentioned before, within this block there are three sub-blocks. Each sub-block is composed by three components: the flash box, the evaporator and the pre-heater. The balances corresponding to the flash box and the pre-heater are the same for the three blocks, but those corresponding to the evaporator are slightly different. Therefore, in each sub-block only the evaporator will be analyzed, and then the flash box and the pre-heater will be analyzed for the three sub-blocks.

*3.2.1 Effects in which the distillate that enters comes from the previous pre-heater*

The effects corresponding to this sub-block are: 2, 5, 8, 11 y 14. Fig 3 shows a schematic diagram of a typical type of this effect.

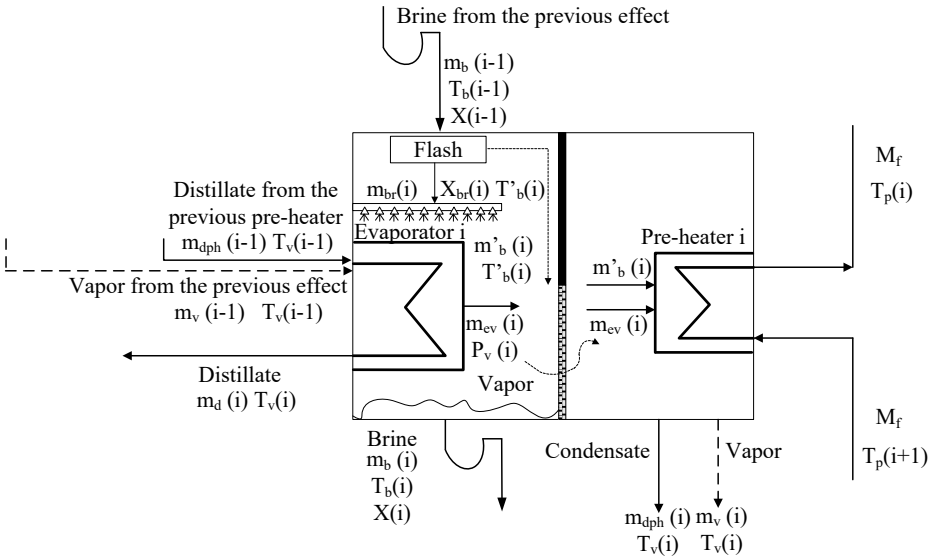


Fig 3. Flow diagram of the effects 2, 5, 8, 11 and 14

The mass, salt and energy balances are the following:

- Energy balance:

$$m_{dph}(i-1) \cdot h_{dph}(i-1) + m_v(i-1) \cdot h_v(i-1) + m_{br}(i) \cdot h_{br}(i) = m_{ev}(i) \cdot h_v(i) + m_b(i) \cdot h_b(i) + m_d(i) \cdot h_d(i) \tag{12}$$

where $m_{dph}(i-1)$ is the distillate mass flow rate coming from the pre-heater i-1, $m_v(i-1)$ is the vapor mass flow rate that leaves the pre-heater i-1 and enters the evaporator i, $m_{br}(i)$ is the brine mass flow rate which is sprayed over the evaporator I bundle tube, $m_b(i)$ is the brine mass flow rate that leaves the evaporator i and $m_d(i)$ is the distillate mass flow rate that leaves the evaporator i.

- Mass and salt balances:

$$m_{br}(i) = m_{ev}(i) + m_b(i) \tag{13}$$

$$m_{br}(i)\cdot X_{br}(i) = m_b(i)\cdot X(i) \tag{14}$$

where $X_{br}(i)$ is the salinity of the brine that is sprayed over the evaporator i bundle tube and $X(i)$ is the brine salinity that leaves the evaporator i.

The distillate coming from the preheater i-1, $m_{dph}(i-1)$ join the condensate generated inside the tubes of the evaporator i, $m_c(i)$, which is produced from the condensation of the vapor coming from the effect i-1, $m_v(i-1)$. Both distillates form the total distillate in the effect i, $m_d(i)$, which leaves the effect as saturated liquid at a temperature of $T_v(i)$ (saturation temperature at the pressure $P_v(i)$):

$$m_d(i) = m_{dph}(i-1) + m_c(i) \tag{15}$$

$$m_c(i) = m_v(i-1) \tag{16}$$

*3.2.2 Effects in which the distillate that enters comes from the previous effect and pre-heater*

The effects corresponding to this sub-block are: 3, 4, 6, 9 and 12. Fig 4 shows a schematic diagram of a typical type of this effect.

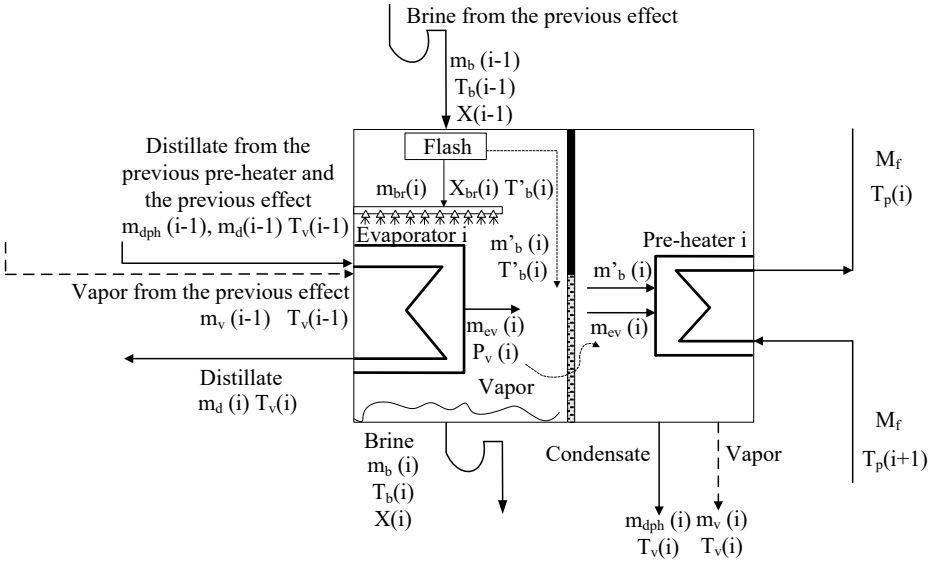


Fig 4. Flow diagram of the effects 3, 4, 6, 9 and 12

The mass, salt and energy balances are the following:

- Energy balance:

$$m_{dph}(i-1)\cdot h_{dph}(i-1) + m_d(i-1)\cdot h_d(i-1) + m_v(i-1)\cdot h_v(i-1) + m_{br}(i)\cdot h_{br}(i) = m_{ev}(i)\cdot h_v(i) + m_b(i)\cdot h_b(i) + m_d(i)\cdot h_d(i) \tag{17}$$

- Mass and salt balances:

$$m_{br}(i) = m_{ev}(i) + m_b(i) \tag{18}$$

$$m_{br}(i)\cdot X_{br}(i) = m_b(i)\cdot X(i) \tag{19}$$

In this case, the distillate coming from the previous effect, $m_d(i-1)$ together with the distillate from the pre-heater i-1, $m_{dph}(i-1)$ join the condensate generated inside the tubes of the evaporator i, $m_c(i)$. Both distillate form the total distillate in this effect, $m_d(i)$, that, as before, leaves the effect as saturated liquid at a temperature of $T_v(i)$.

$$m_d(i) = m_d(i-1) + m_{dph}(i-1) + m_c(i) \tag{20}$$

$$m_c(i) = m_v(i-1) \tag{21}$$

*3.2.3 Effects in which the distillate that enters comes from the previous effect, from the previous pre-heater and from further effects*

The effects corresponding to this sub-block are: 7, 10 and 13. Fig 5 shows a schematic diagram of a typical type of this effect.

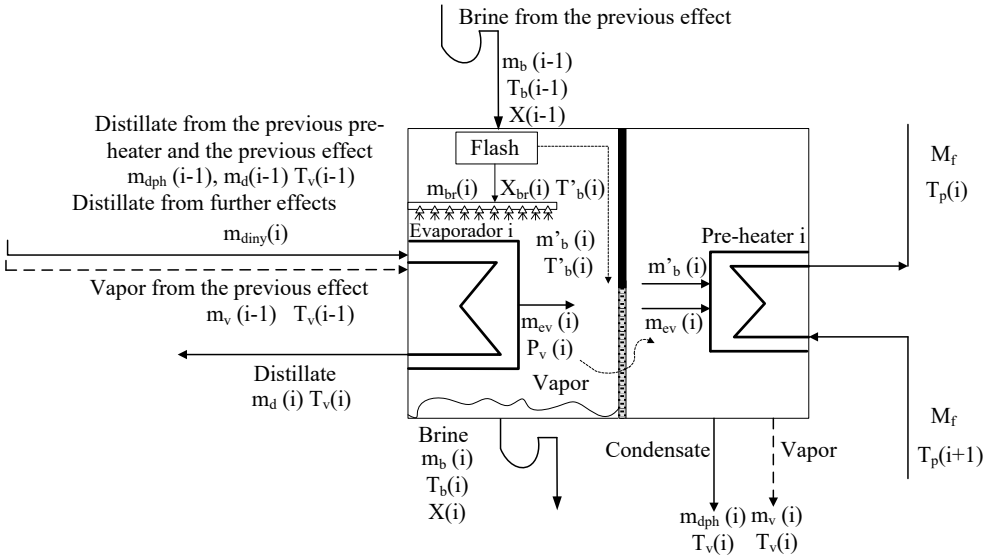


Fig 5. Flow diagram of the effects 7, 10 and 13

The mass, salt and energy balances are the following:

- Energy balance:

$$m_{dph}(i-1)\cdot h_{dph}(i-1) + m_d(i-1)\cdot h_d(i-1) + m_{diny}(i)\cdot h_{diny}(i) + m_v(i-1)\cdot h_v(i-1) + m_{br}(i)\cdot h_{br}(i) = m_{ev}(i)\cdot h_v(i) + m_b(i)\cdot h_b(i) + m_d(i)\cdot h_d(i) \tag{22}$$

- Mass and salt balances:

$$m_{br}(i) = m_{ev}(i) + m_b(i) \tag{23}$$

$$m_{br}(i)\cdot X_{br}(i) = m_b(i)\cdot X(i) \tag{24}$$

In this case, the distillate coming from the previous effect, $m_d(i-1)$ together with the distillate from the pre-heater i-1 and with part of the distillate from further effects, $m_{diny}(i-1)$ join the condensate generated inside

the tubes of the evaporator i, $m_c(i)$. The three distillates form the total distillate in this effect, $m_d(i)$, that, as in the previous cases, leaves the effect as saturated liquid at a temperature of $T_v(i)$.

$$m_d(i) = m_d(i-1) + m_{dph}(i-1) + m_{diny}(i) + m_c(i) \tag{25}$$

$$m_c(i) = m_v(i-1) \tag{26}$$

The distillate mass flow rate that enters the effects 7, 10 and 13, $m_{diny}(i)$, is determined by taking into account that the sum of distillate volumetric flow rate from the previous effect and this one of the distillate that enters the effects 7, 10 and 13 is equal to 0.24 $m^3/h$.This volumetric flow rate ensures that the rest of tubes are enough to get a suitable velocity of the vapor for the condensation process.

Fig 6 shows a flow diagram of the inlet and outlet distillate streams between the fourth and fourteenth effects. Energy and mass balances are shown bellow. They will be useful to determine the distillate temperature at the outlet of the mixers and the total distillate that leaves the effects 2 – N.

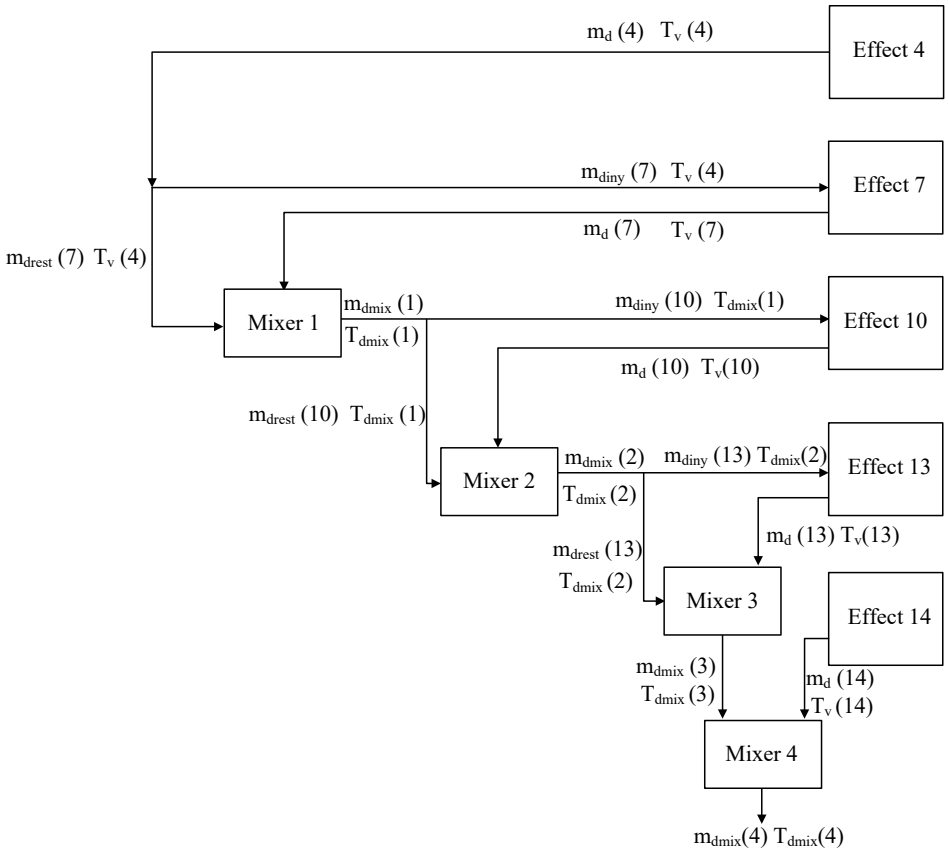


Fig 6: Flow diagram of the extractions and injections of distillate in the effects

The mass and energy balances through the mixers are shown bellow:

Mixer 1:

$$m_{dmix}(1) = m_{drest}(7) + m_d(7) \tag{27}$$

$$m_{drest}(7) = m_d(4) - m_{diny}(7) \tag{28}$$

$$m_{dmix}(1)\cdot h_{dmix}(1) = m_{drest}(7)\cdot h_{drest}(7) + m_d(7)\cdot h_d(7) \tag{29}$$

Mixer 2:

$$m_{dmix}(2) = m_{drest}(10) + m_d(10) \tag{30}$$

$$m_{drest}(10) = m_{dmix}(1) - m_{diny}(10) \tag{31}$$

$$m_{dmix}(2)\cdot h_{dmix}(2) = m_{drest}(10)\cdot h_{drest}(10) + m_d(10)\cdot h_d(10) \tag{32}$$

Mixer 3:

$$m_{dmix}(3) = m_{drest}(13) + m_d(13) \tag{33}$$

$$m_{drest}(13) = m_{dmix}(2) - m_{diny}(13) \tag{34}$$

$$m_{dmix}(3)\cdot h_{dmix}(3) = m_{drest}(13)\cdot h_{drest}(13) + m_d(13)\cdot h_d(13) \tag{35}$$

Mixer 4:

$$m_{dmix}(4) = m_{dmix}(3) + m_d(14) \tag{36}$$

$$m_{dmix}(4)\cdot h_{dmix}(4) = m_{dmix}(3)\cdot h_{dmix}(3) + m_d(14)\cdot h_d(14) \tag{37}$$

It is considered that the distillate leaves each effect as saturated liquid at the same temperature of the vapor inside the effect, $T_v(i)$.

As in the first effect, the temperature of the vapor generated in the effect i, $T_v(i)$, is lower that of the boiling brine temperature in such effect ($T_b(i)$) by the boiling point elevation ($BPE$)i:

$$T_b(i) = T_v(i) + (BPE)_i \tag{38}$$

The $(BPE)_i$ is determined by the Eq. (7).

The heat transfer equation for a typical evaporator i can be written as follows:

$$Q_{ev}(i) = U_{ev}(i)A_{ev}(i)\cdot(T_v(i-1) - T_b(i)) \tag{39}$$

where $U_{ev}(i)$ is the overall heat transfer coefficient of a typical evaporator i and $A_{ev}(i)$ is the evaporator i bundle tube, that is the same for all the evaporators from 2 to N. $Q_{ev}(i)$ is the thermal power that is transferred from the vapor coming from the previous effect (i-1) to the seawater sprayed over the bundle tube of the effect i. It is given by:

$$Q_{ev}(i) = m_v(i-1)\cdot\lambda_v(i-1) \tag{40}$$

where $\lambda_v(i-1)$ is the latent heat of formed vapor at a temperature of $T_v(i-1)$.

In the cases of the control volumes flash and pre-heater, the mass and energy balances are the same for the three sub-blocks, and they are shown bellow.

**Flash:**

The brine coming from the previous effect, $m_b(i-1)$, enters the effect i which is at a lower pressure and a portion of vapor is formed by flashing, decreasing its temperature from $T_b(i-1)$ to $T'_b(i)$. This temperature is higher than the boiling temperature within the effect I, Tb(i) by the non-equilibrium allowance, which is a measure of the flashing process [5]:

$$T_b^{'}(i) = T_b(i) + (NEA)_i \tag{41}$$

This parameter can be determined by the following correlation [20]:

$$(NEA)_i = 33(\Delta T_b(i))^{0,55} / T_v(i) \tag{42}$$

where $\Delta T_b(i)$ is:

$$\Delta T_b(i) = T_b(i-1) - T_b(i) \tag{43}$$

From the flashing evaporation an amount of vapor is obtained, $m'_b(i)$ that join in the way to the pre-heater the vapor generated by boiling, $m_{ev}(i)$. The rest non-evaporated brine, $m_{br}(i)$ is sprayed over the evaporator bundle tube. The energy, mass and salts balances are shown bellow.

- Energy balance:

$$m_b(i-1)\cdot h_b(i-1) = m_{br}(i)\cdot h_{br}(i) + m_b^{'}(i)\cdot h_b^{'}(i) \tag{44}$$

- Mass and salts balances:

$$m_b(i-1) = m_{br}(i) + m_b^{'}(i) \tag{45}$$

$$m_b(i-1)\cdot X(i-1) = m_{br}(i)\cdot X_{br}(i) \tag{46}$$

**Pre-heater:**

The energy and mass balances are shown bellow.

- Energy balance:

$$m_{ev}(i)\cdot h_{ev}(i) + m_b^{'}(i)\cdot h_b^{'}(i) + M_f\cdot h_p(i+1) = m_v(i)\cdot h_v(i) + m_{dph}(i)\cdot h_{dph}(i) + M_f\cdot h_p(i) \tag{47}$$

In the case of the last pre-heater ($i=N-1$) the seawater inlet temperature is the seawater outlet temperature from the condenser, $T_{cw,out}$, so the energy balance can be written as follows:

$$m_{ev}(N-1)\cdot h_{ev}(N-1)+m_b^{'}(N-1)\cdot h_b^{'}(N-1)+M_f\cdot h_{cw,out}=m_v(N-1)\cdot h_v(N-1) \\ +m_{dph}(N-1)\cdot h_{dph}(N-1)+M_f\cdot h_p(N-1) \tag{48}$$

- Mass balance:

$$m_{ev}(i)+m_b^{'}(i)=m_v(i)+m_{dph}(i) \tag{49}$$

The heat transfer equation for a typical pre-heater $i$ is written as follows:

$$Q_p(i)=A_p(i)\cdot U_p(i)\cdot\frac{\left(T_v(i)-T_p(i+1)\right)-\left(T_v(i)-T_p(i)\right)}{\ln\left(\frac{T_v(i)-T_p(i+1)}{T_v(i)-T_p(i)}\right)} \tag{50}$$

where $U_p(i)$ is the overall heat transfer coefficient for a typical pre-heater, $A_p(i)$ is the pre-heater bundle of a pre-heater (it is the same for all the pre-heaters) and $Q_p(i)$ is the thermal power that is transferred from the vapor coming from the evaporator i to the seawater flowing through the pre-heater bundle tube. It is determined as follows:

$$Q_p(i)=M_f\cdot(h_p(i)-h_p(i+1)) \tag{51}$$

In the case of the last pre-heater, the heat transfer equation is given by:

$$Q_p(N-1)=A_p(N-1)\cdot U_p(N-1)\cdot\frac{\left(T_v(N-1)-T_{cw,out}\right)-\left(T_v(N-1)-T_p(N-1)\right)}{\ln\left(\frac{T_v(N-1)-T_{cw,out}}{T_v(N-1)-T_p(N-1)}\right)} \tag{52}$$

where $Q_p(N-1)$ is written as follows:

$$Q_p(N-1)=M_f\cdot(h_p(N-1)-h_{cw,out}) \tag{53}$$

The temperature difference across the effects ($\Delta T_v$) and the pre-heaters ($\Delta T_p$) is calculated by the following expressions:

*Evaporators*:

$$\Delta T_v=\frac{T_v(1)-T_v(N)}{N-1} \tag{54}$$

Then, the vapor temperature in each evaporator, $T_v(i)$, is determined as follows:

$$T_v(i) = T_v(i-1) - \Delta T_v \tag{55}$$

*Pre-heaters*:

$$\Delta T_p = \frac{T_f - T_{cw,out}}{N-1} \tag{56}$$

Therefore, the seawater temperature in each pre-heater is determined as follows:

$$T_p(i) = T_p(i+1) + \Delta T_p \tag{57}$$

*3.3 The end condenser*

The end condenser (see the flow diagram in Fig 7) is located next to the last effect of the plant ($i=N$), so the vapor generated in this effect flows to the condenser through the demister and releases its latent heat to the seawater flowing through the bundle tube. Therefore, the vapor condenses and the seawater increases its temperature.

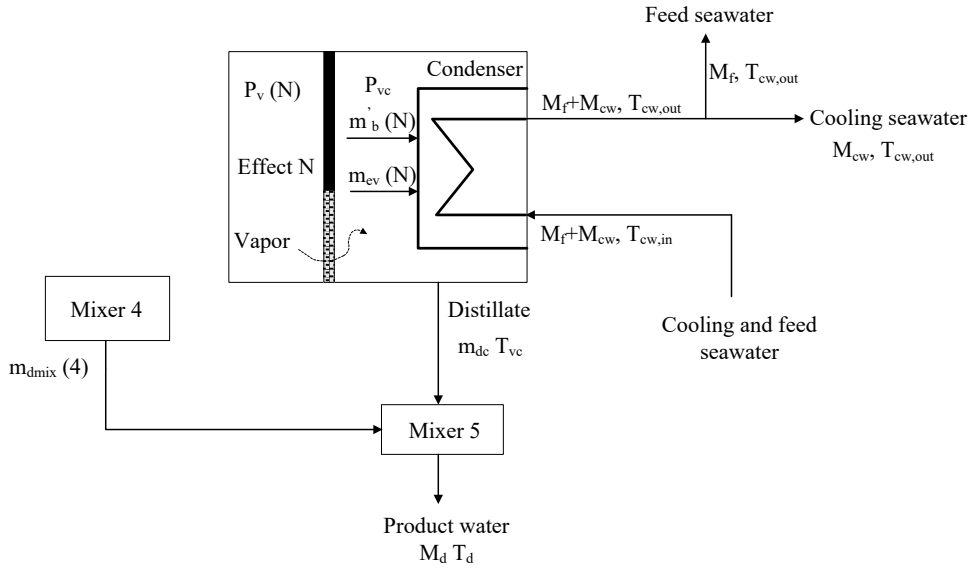


Fig 7. Flow diagram of the end condenser

The mass, salt and energy balances are the following:

- Energy balance:

$$m'_b(N)\cdot h'_b(N) + m_{ev}(N)\cdot h_{ev}(N) + (M_f + M_{cw})\cdot h_{cw,in} = (M_f + M_{cw})\cdot h_{cw,out} + m_{dc}\cdot h_{vc} \tag{58}$$

where $M_{cw}$ is the cooling seawater mass flow rate.

Since negligible heat losses to the surroundings have been considered, the vapor temperature inside the effect N, $T_v(N)$, is set to be the same as the vapor temperature in the condenser, $T_{vc}$ (it corresponds to the saturation pressure, $P_{vc}$).

- Mass balance:

$$m_{dc} = m_{ev}(N) + m_b^{'}(N) \tag{59}$$

Finally, the product water of the plant, $M_d$ and its temperature, $T_d$, are determined by a mass and energy balance in the Mixer 5:

- Mass balance:

$$M_d = m_{dc} + m_{dmix}(4) \tag{60}$$

- Energy balance:

$$m_{dmix}(4) \cdot h_{dmix}(4) + m_{dc} \cdot h_{dc} = M_d \cdot h_d \tag{61}$$

On the other hand, the heat transfer equation of the end condenser is given by:

$$Q_c = A_c \cdot U_c \frac{\left(T_v(N) - T_{cw,in}\right) - \left(T_v(N) - T_{cw,out}\right)}{\ln\left(\frac{T_v(N) - T_{cw,in}}{T_v(N) - T_{cw,out}}\right)} \tag{62}$$

where $U_c$ is the overall heat transfer coefficient of the condenser, $A_c$ is the condenser bundle and $Q_c$ is the thermal power transferred from the vapor coming from the last effect to the feed and cooling seawater flowing through the condenser bundle tube. It is written as follows:

$$Q_c = (M_f + M_{cw}) \cdot (h_{cw,out} - h_{cw,in}) \tag{63}$$

The model described above is useful to determine the Performance Ratio (*PR*) of the plant, which is defined as kg of distillate produced for every 2326 kJ of thermal energy supplied to the system. Therefore, the equation to assess it is:

$$PR = \frac{M_d}{Q_h} \times \frac{2326kJ}{1kg} \tag{64}$$

**4. Parameterization**

In the equations described above there are a series of variables, that are: the overall heat transfer coefficient for the first effect ($U_h$), the overall heat transfer coefficient for the pre-heaters ($U_p(i)$), the vapor temperature inside the first effect, ($T_v(1)$) and the cooling seawater outlet temperature ($T_{cwout}$), whose value is needed to determine in order to run the model. For this purpose, a series of parametric equations that represent these variables have been obtained from a three-level factorial experimental design ($3^k$), The variables or factors ($k$) with the actual levels of operation (low (-1), medium (0) and high (+1)) are shown in Table 3. therefore, a experimental campaign have been performed with a total of 81 ($3^4$) experiments.

Table 3
Variable factors and their actual values of operation

| | Symbol | -1 | 0 | +1 |
|---|---|---|---|---|
| Last effect vapor temperature (°C) | $T_v(14)$ | 25 | 30 | 35 |
| Heating water inlet temperature (°C) | $T_{h,in}$ | 65 | 70 | 75 |
| Feed seawater flow ($m^3/h$) | $M_f$ | 6 | 7 | 8 |
| Heating water flow (L/h) | $M_h$ | 7 | 9.5 | 12 |

The experiments were performed in 10 months, from March to January and they were designed taking into account that the last effect vapor temperature has to be higher that the minimum seawater temperature in the Mediterranean Sea (that is 15 ºC) plus a temperature difference of 10 ºC in the condenser in order to satisfy the cooling flow rates required.

The overall heat transfer coefficient for the first effect is obtained from the Eq. (8). However, for the pre-heaters an overall heat transfer coefficient, $\overline{U}_p$ is calculated by considering the total heat transfer, $Q_p$ in all *N-1* pre-heaters:

$$\overline{U}_p = \frac{Q_p}{A_p \cdot \Delta T_p \cdot (N-1)} \tag{65}$$

The total heat transfer rate in the *N-1* pre-heaters is assessed as follows:

$$Q_p = M_f \cdot (h_f - h_{cw,out}) \tag{66}$$

A 2nd order response surface model (Response Surface Methodology, RSM) has been used in order to obtain the parametric equations. Each response has been linked to the factors by a 2nd order polynomial model with interactions as shown in the following equation [21]:

$$Y = \beta_o + \sum_{i=1}^{k} \beta_i X_i + \sum_{i=1}^{k} \beta_{ii} X_i^2 + \sum_{i=1}^{k-1} \sum_{\substack{j=2 \\ j>i}} \beta_{ij} X_i X_j + \varepsilon \tag{67}$$

where $Y$ is the response, $\beta_o$, $\beta_1$,…. $\beta_k$, $\beta_{ij}$ are the regression coefficients, $X_i$, $X_j$ (j=i+1, …,$k$) represent the independent variables or factors (last effect vapor temperature, $T_v(14)$, heating water inlet temperature, $T_{h,in}$, feed seawater flow, $M_f$, and heating water flow, $M_h$) and $\varepsilon$ is the statistical error.

The RSM model coefficients for each response are computed by multiple linear regression (MLR) method ([21, 22]):

$$\beta = (X^T X)^{-1} X^T Y \tag{68}$$

where ~~$\beta$~~ is the vector formed by the regression coefficients, $X$ is the matrix ($N \times u$) of the independent variables, $u$ is the number of regression coefficients in the RS-model (Eq. (67)) an Y is a vector ($N \times 1$) formed by the responses of the N experiments. According to this method the β are determined by the method of least squares. In other words, the β values are chosen in order to minimize the sum of squared residuals.~~β coefficients are determined by the method of least squares. In other words, the $\beta$ values are chosen in order to minimize the sum of squared residuals.~~

For each response variable, the parametric equations with the corresponding regression coefficients have been determined.

## 5. Results and discussion

The independent and dependent variables are fitted to the 2nd order model equation (Eq. (67)) and for each response variable is examined the goodness of fit. It and the significance of each regression coefficient were obtained using the *Modde 5.0* software with a confidence level of 95 %. Table 4 and Table 5 present the regression relationships for each response monitored and the $p$ values. They are used as a tool to check the significance of each of the coefficients, which in turn may indicate the pattern of the interaction between the variables. The smaller the value of $p$, the more significant is the corresponding coefficient [23].

Table 4:
Test of significance for the response variable $T_v(1)$ and $T_{cw,out}$ regression coefficients

| | $T_v$ (1) | | $T_{cw,out}$ | |
|---|---|---|---|---|
| Model term | Coefficient estimate | *p*-Value | Coefficient estimate | *p*-Value |
| $T_v(N)$ | -0.460 | <0.05 | 1.308 | <0.05 |
| $T_{hin}$ | -1.295 | <0.05 | 0.470 | <0.05 |
| $M_f$ | 7.725 | <0.05 | 0.172 | 0.1273 |
| $M_h$ | 0.798 | <0.05 | -0.051 | <0.05 |
| $T_v(N) \cdot T_v(N)$ | -0.005 | 0.2022 | 0.004 | <0.05 |
| $T_{hin} \cdot T_{hin}$ | 0.011 | <0.05 | -0.002 | <0.05 |
| $M_f \cdot M_f$ | 0.679 | 0.5778 | 0.212 | 0.4544 |
| $M_h \cdot M_h$ | 0.052 | <0.05 | 0.009 | <0.05 |
| $T_v(N) \cdot T_{hin}$ | 0.015 | <0.05 | -0.006 | <0.05 |
| $T_v(N) \cdot M_f$ | -0.056 | 0.2694 | -0.021 | 0.0720 |
| $T_v(N) \cdot M_h$ | -0.009 | 0.1212 | $3.517 \cdot 10^{-3}$ | 0.8013 |
| $T_{hin} \cdot M_f$ | -0.060 | 0.2508 | -0.003 | 0.7984 |
| $T_{hin} \cdot M_h$ | 0.013 | <0.05 | -0.001 | 0.3075 |
| $M_f \cdot M_h$ | -0.013 | 0.8967 | -0.024 | 0.3117 |

Table 5
Test of significance for the response variable $U_h$ and $U_p$ regression coefficients

| | $U_h$ | | $U_p$ | |
|---|---|---|---|---|
| Model term | Coefficient estimate | *p*-value | Coefficient estimate | *p*-value |
| $T_v(N)$ | -0.478 | <0.05 | $-8.114 \cdot 10^{-4}$ | 0.4614 |
| $T_{hin}$ | -1.353 | <0.05 | $1.824 \cdot 10^{-4}$ | 0.2099 |
| $M_f$ | 1.000 | 0.4903 | 0.838 | <0.05 |

| | | | | |
|---|---|---|---|---|
| $M_h$ | 0.463 | <0.05 | $-7.177\cdot10^{-4}$ | 0.9957 |
| $T_v(N)\cdot T_v(N)$ | -0.001 | 0.2106 | $1.205\cdot10^{-5}$ | 0.1451 |
| $T_{hin}\cdot T_{hin}$ | 0.008 | <0.05 | $-3.321\cdot10^{-6}$ | 0.7024 |
| $M_f\cdot M_f$ | -0.065 | 0.8385 | $-2.121\cdot10^{-4}$ | 0.9324 |
| $M_h\cdot M_h$ | -0.008 | 0.1079 | $-2.769\cdot10^{-5}$ | 0.4586 |
| $T_v(N)\cdot T_{hin}$ | 0.008 | <0.05 | $3.978\cdot10^{-6}$ | 0.5626 |
| $T_v(N)\cdot M_f$ | -0.006 | 0.6662 | $-1.319\cdot10^{-4}$ | 0.2087 |
| $T_v(N)\cdot M_h$ | -0.002 | 0.3157 | $5.453\cdot10^{-6}$ | 0.6590 |
| $T_{hin}\cdot M_f$ | -0.007 | 0.6168 | $3.738\cdot10^{-5}$ | 0.7267 |
| $T_{hin}\cdot M_h$ | -0.003 | 0.0811 | $1.321\cdot10^{-5}$ | 0.3011 |
| $M_f\cdot M_h$ | -0.006 | 0.8054 | $7.617\cdot10^{-5}$ | 0.7119 |

The following regression equations represent the best description of the variables $T_v(1)$, $T_{cw,out}$, $U_h$ y $U_p$ after the elimination of non-significant parameters (p>0.05) from the results summarized in Table 4 and Table 5:

$$T_v(1) = 85.9763 - (1.06873\cdot T_v(N)) - (1.20385\cdot T_{h,in}) - (0.974267\cdot M_f) + (1.43293\cdot M_h) + (0.0104179\cdot T_{h,in}^2) - (0.055331\cdot M_h^2) + (0.017083\cdot T_v(N)\cdot T_{h,in}) \quad (69)$$

$$T_{cw,out} = -19.8783 + (1.27265\cdot T_v(N)) + (0.432938\cdot T_{h,in}) - (0.193712\cdot M_h) + 0.00391375\cdot T_v^2(N)) - (0.00199305\cdot T_{h,in}^2) + (0.00936997\cdot M_h^2) - (0.00632534\cdot T_v(N)\cdot T_{h,in}) \quad (70)$$

$$U_h = 25.1217 - (0.0992825\cdot T_v(N)) - (0.678212\cdot T_{h,in}) + (0.30056\cdot M_h) - (0.00323972\cdot T_v^2(N)) + (0.00392379\cdot T_{h,in}^2) - (0.0112135\cdot M_h^2) + (0.00442078\cdot T_v(N)\cdot T_{h,in}) \quad (71)$$

$$U_p = -0.000540399 + (0.836569\cdot M_f) \quad (72)$$

The goodness of fit of the model is evaluated by the coefficient of determination ($R^2$). It is defined as the proportion of variation in the response attributed to the model. It is suggested that $R^2$ should be closed to 1 for a good fit model [24]. However, a large value of $R^2$ does not always imply that the regression model is a good one. $R^2$ always increases with the addition of a new variable to the model, regardless of weather additional variable is statistically significant or not [25]. Thus, it is preferred to use the adjusted-$R^2$ to evaluate the model adequacy since it is adjusted for the number of terms in the model. The adjusted-$R^2$ should be over 90 % indicating a high degree of correlation between the observed and predicted values [25]. Besides these coefficients, another one to evaluate the goodness of fit of the model is the coefficient $Q^2$, which is defined as the fraction of variation of the response that can be predicted by the model. Values of $Q^2$ close to 1 indicate a very good model [26]. Table 6 summarizes the statistics used to test the adequacy of the model. The results indicate that all the fit indices show a good fit to the estimated models for all the variables ($T_v(1)$, $T_{cw,out}$, $U_h$ and $U_p$).

Table 6
Statistics used to test goodness of fit of the models

| | $T_v(1)$ | $T_{cw,out}$ | $U_h$ | $U_p$ |
|---|---|---|---|---|
| $R^2$ | 0.984 | 0.999 | 0.940 | 0.999 |

| | | | | |
|---|---|---|---|---|
| Adjusted-$R^2$ | 0.983 | 0.999 | 0.934 | 0.999 |
| $Q^2$ | 0.980 | 0.998 | 0.924 | 0.998 |

## 6. Conclusions

A mathematical model of an MED plant has been developed and validated with experimental data obtained from an MED pilot plant located at the PSA. In order to run the model a series of parametric equations have been determined using a $3^4$ factorial design with a total of 81 experiments. The variable factors were varied using a wide operational range (varying the last effect vapor temperature from 25 ºC to 35 ºC, the heating water inlet temperature in the range of 65 ºC to 75 ºC, the feed water flow from 6 $m^3$/h to 8 $m^3$/h and the heating water flow in the range of 7-10 L/s). The developed model equations can be used to predict the overall heat transfer coefficient for the first effect ($U_h$), the overall heat transfer coefficient for the pre-heaters ($U_{p(i)}$), the vapor temperature inside the first effect, ($T_{v(1)}$) and the cooling seawater outlet temperature ($T_{cwout}$), as influenced by operating factors studied in this system. The results showed a good agreement between the predicted and experimental data for all the variables, with a $R^2$, Adjusted-$R^2$ and $Q^2$ higher than 90 %.

## References


[1] X. Wang, et al. Low grade heat driven multi-effect distillation technology. Int. J. Heat Mass Transfer 54 (2011) 5497-5503.

[2] E. Mathioulakis, V. Belessiotis and E. Delyannis. Desalination by using alternative energy: Review and state-of-the-art. Desalination 203 (2007) 346-365.

[3] G. Lourdes. Renewable energy applications in desalination: state of the art. Solar Energy 75 (2003) 381-393.

[4] L. García-Rodríguez. Seawater desalination driven by renewable energies: a review. Desalination 143 (2002) 103-113.

[5] H. El-Dessouky, I. Alaitiqi, S. Bingulac and H. Ettouney. Steady-Stete Analysis of the Multiple Effect Evaporation Desalination Process. Quemical Engineering and Technology 21 (1998) 437-451.

[6] H.T. El-Dessouky and H.M. Ettouney. Multiple-effect evaporation desalination systems. thermal analysis. Desalination 125 (1999) 259-276.

[7] A.M. El-Nashar and A.A. Qamhiyeh. Simulation of the steady-state operation of a multi-effect stack seawater distillation plant. Desalination 101 (1995) 231-243.

[8] A.M. El-Nashar. Predicting part load performance of small MED evaporators - a simple simulation program and its experimental verification. Desalination 130 (2000) 217-234.

[9] R.K. Kamali, A. Abbassi and S.A. Sadough Vanini. A simulation model and parametric study of MED–TVC process. Desalination 235 (2009) 340-351.

[10] A. Trostmann. Improved approach to steady state simulation of multi-effect distillation plants. 7 (2009) 93-110.

[11] G. Gautami and S. Khanam. Selection of optimum configuration for multiple effect evaporator system. Desalination 288 (2012) 16-23.

[12] P. Palenzuela, et al. Modeling of the heat transfer of a solar multi-effect distillation plant at the Plataforma Solar de Almería. Desalination and Water Treatment 31 (2011) 257-268.

[13] E. Zarza, (Ed.), Solar Thermal Desalination Project, First Phase Results and Second Phase Description, CIEMAT, Madrid, Spain, 1991.

[14] E. Zarza. Solar Thermal Desalination Project Phase II Results & Final Project Report. (1994)

[15] D. Alarcón-Padilla and L. García-Rodríguez. Application of absorption heat pumps to multi-effect distillation: a case study of solar desalination. Desalination 212 (2007) 294-302.

[16] D. Alarcón-Padilla, L. García-Rodríguez and J. Blanco-Gálvez. Assessment of an absorption heat pump coupled to a multi-effect distillation unit within AQUASOL project. Desalination 212 (2007) 303-310.

[17] D. Alarcón-Padilla, et al. First experimental results of a new hybrid solar/gas multi-effect distillation system: the AQUASOL project. Desalination 220 (2008) 619-625.
[18] D.C. Alarcón-Padilla, L. García-Rodríguez and J. Blanco-Gálvez. Experimental assessment of connection of an absorption heat pump to a multi-effect distillation unit. Desalination 250 (2010) 500-505.
[19] H. El-Dessouky, H. Ettouney, I. Alatiqi and G. Al-Nuwaibit. Evaluation of steam jet ejectors. Chem. Eng. Process 41 (2002) 551-561.
[20] H. El-Dessouky and H. Ettouney, (Eds.), Fundamentals of Salt Water Desalination, ELSEVIER SCIENCE B.V, Amsterdam, The Netherlands, 2002.
[21] M. Khayet, et al. Optimization of solar-powered reverse osmosis desalination pilot plant using response surface methodology. Desalination 261 (2010) 284-292.
[22] D.C. Montgomery and R.H. Myers, (Eds.), Reponse Surface Methodology: Process and Product in Optimization using Designed Experiments, John Wiley & Sons, New York, 1995.
[23] A. Haber and R. Runyon, (Eds.), General Statistics, third ed. John Wiley & Sons Inc., New York, 1977.
[24] F. Xiangli, et al. Optimization of preparation conditions for polydimethylsiloxane (PDMS)/ceramic composite pervaporation membranes using response surface methodology. J. Membr. Sci. 311 (2008) 23-33.
[25] P. Onsekizoglu, K. Savas Bahceci and J. Acar. The use of factorial design for modeling membrane distillation. J. Membr. Sci. 349 (2010) 225-230.
[26] B. George E.P, H. J.Stuart and H. William Gordon, (Eds.), Statistics for Experimenters: An Introduction to Design, Data Analysis and Model Building, Ed.Wiley, New York, 1978.